2022 IEEE International Symposium on Antennas and Propagation and USNC-URSI Radio Science Meeting (AP-S/USNC-URSI) | 978-1-6654-9658-2/22/$31.00 ©2022 IEEE | DOI: 10.1109/AP-S/USNC-URSI47032.2022.9887248

A Versatile Polynomial Model for Reflection by a Reflective Intelligent Surface with Varactors

David Hanna[(1)], Miguel Saavedra Melo[(1)], Feiyu Shan[(1)], and Filippo Capolino[(1)(2)]

[(1)] Dept. of Electrical Engineering and Comp. Science, University of California, Irvine, CA 92617, USA
[(2)] Department of Communications and Signal Theory, University Carlos III of Madrid, Spain

***Abstract*—An analytical model for reflection of a reconfigurable intelligent surface (RIS) using varactors to adjust the reflection phase of an incident plane wave is presented. The model results are compared to a full-wave RIS simulation for different varactor bias voltages. The model is intended to be analytical and simple enough, but related to a realistic RIS, to be inserted into MIMO wireless systems algorithms to estimate the propagation channel including the RIS.**

I. Introduction

Reconfigurable Intelligent Surfaces (RIS) are metasurfaces that can be reconfigured by using external signal [1]. In the context of wireless communications, RIS have been proposed as a suitable solution to maximize the spectral and energy efficiency of wireless systems at a low cost [2] by establishing favorable channel responses to through the wireless propagation control environment [3], [4]. Here, we consider an RIS that uses varactors to tune the reflection phase of the reflected wave with the capability to provide suitable phase gradients to reflect the signal to desired directions. The RIS should direct the signal received from the nearest wireless tower to various users at different locations, and vice versa. We present a manufacture-friendly RIS and model its performance by providing an analytical model that can be used in the algorithms that model wireless communications. The RIS equivalent reflection model is obtained by resorting to a physics-based equivalent circuit, including any possible varactor model. Currently simplified RIS models are utilized in wireless system modeling [5]. The RIS model discussed here is based on a good approximation to the full-wave simulations and is a first step toward using a realistic RIS model to improve wireless system simulations [2], [6].

II. RIS and Its Model

The metasurface design provides a programmable reflection phase shift on its surface. For simplicity we only show here the case of normally incident plane wave polarized in the x-direction, Fig. 1, to steer or reflect to different directions. The RIS element is here chosen to be a dogbone, or H shaped, patterned metal on a grounded dielectric substrate. Varactors are attached between adjacent dogbones. The RIS element behavior replicates the metasurface made of dogbones in [8]. Indeed, it is the so called magnetic resonance that is responsible of providing the tunability of the reflection coefficient phase. The geometry is shown in Fig. 1. This design uses RO4350B as dielectric spacer, with relative permittivity $\epsilon_r = 3.55$ and tan $\delta = 0.0037$, and the dimensions, in mm, are: $A = B = 4.1$, $A1 = 1$, $A2 = 3.7$, $B1 = 2$, $B2 = 1$, $H = 3$, and $G = 0.4$. The device used here to allow a reconfigurable behavior is a varactor diode arranged in the middle of the structure and joining the two parts of the dogbone that are separated by the gap. In this work we show the features obtained by using the SMV2019-079LF varactor, given its low series induntance of 0.7 nH and resistance which are important for this design. The capacitance tuning range is limited to 0.22 - 0.5 pF. In order to know the performance, the commercial software CST Studio Suite based on the finite elements method was used to obtain the reflection coefficient by full-wave simulations, including the effect of the varactor as a lumped load. The magnitude and phase of the reflection coefficient for various varactor reverse bias voltages are plotted in Fig. 2. In Fig. 3 the phase shift is plotted for three different frequencies as a function of the varactor bias voltage, showing the reconfiguration of the RIS. We use the equivalent circuit

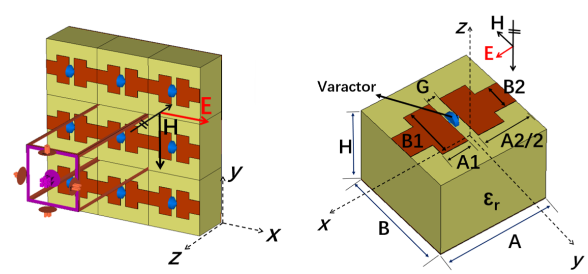

Fig. 1. RIS formed by a periodic arrangement of dogbone-shaped conductors on a grounded dielectric substrate, and unit cell with geometrical parameters. The polarization of the incident electric field is along x.

model shown in Fig. 4 to represent the RIS and evaluate the reflection coefficient [6], [7]. The parameters R_d, C_d and L_d are the resistance, capacitance, and inductance associated with the dogbone unit cell element, respectively. The inductance L_s is an equivalent element that account for the substrate, and may contain also nonlinear terms in ω. The varactor is represented by the series $R_v(V)$, $C_v(V)$, and L_v, where V is the varactor voltage. The effective varactor capacitance in the circuit is $C_{eff}(\omega, V) = C_v / \left(1 - \omega^2 C_v L_v\right)$. The fractional polynomial expression of the reflection coefficient at the surface level is evaluated by using the equivalent RIS impedance of the equivalent lumped circuit in Fig. 4. Excluding for a moment the varactor, the RIS impedance is given by

$$Z_{RIS} = \frac{j\omega L_s \left(1 + j\frac{\omega L_d}{R_d} - \omega^2 L_d C_d\right)}{1 + j\frac{\omega(L_d + L_s)}{R_d} - \omega^2 (L_d + L_s) C_d}. \quad (1)$$

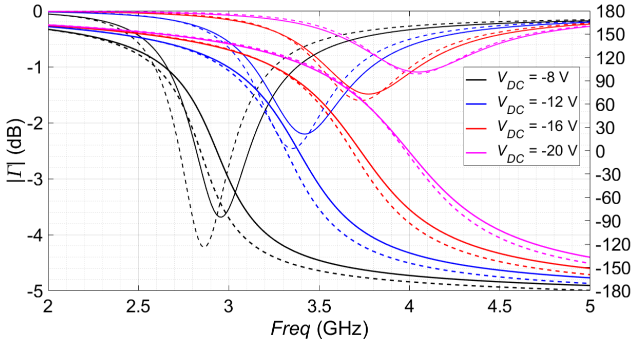

Fig. 2. Magnitude and phase of the RIS reflection coefficient calculated using the circuit analytical model (solid lines), and compared with the results of the full-wave simulation (dashed lines).

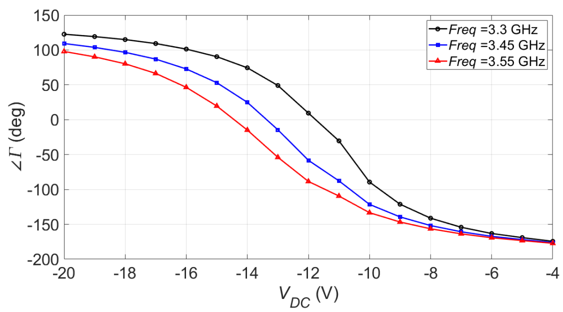

Fig. 3. Reflection coefficient phase of the structure for biasing voltages of the varactor from -20 V to -4 V.

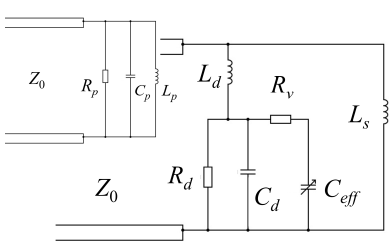

Fig. 4. Equivalent circuital model of the RIS. Z_{RIS} is seen from the left. The inset represents an approximation that describes the "magnetic resonance", i.e., the main feature to manipulate the phase of the reflection coefficient.

A single full-wave simulation is performed to obtain the elements L_d, C_d, and R_d of (1), from the phase reflection curves without initially including the varactor. L_s is determined analytically from the dielectric substrate height and relative dielectric constant. The varactor circuit model in parallel of C_d is analtytically calculated for various varactor voltages, from the datasheet provided by the varactor manufacturer. Therefore, the RIS impedance is still described by (1) after substitution of $C_{d,eff}(V)$ in place of C_d, that accounts for the varactor element. Note that the "magnetic resonance" behavior of the complicated circuit model can be accounted for and reduced to a parallel RLC circuit as shown in the inset of Fig. 4. The reflection phase and magnitude (dB) are shown in Fig. 2, for various varactor voltages. The capability to tune the frequency response (phase reflection) between 3 and 4 GHz is shown.

III. Conclusion and Discussion

The analytical model presented here matches closely with the full-wave simulations of a realistic RIS. The analytical lumped circuit model can be determined from a single full-wave simulation (all frequencies) to extract the metasurface parameters. Subsequently an analytical but accurate model of a realistic varactor is implemented to simulate the reflection phase of the RIS, for varying varactor voltage. By properly choosing the various varactor voltages the RIS can be configured to direct a beam into multiple directions. This simple model can be effectively used in MIMO wireless system algorithms to estimate the performance of realistic RIS. The RIS equivalent circuit parameters extracted using the full-wave simulations account for the periodicity, therefore they are accurate if we assume that the surface gradient of the reflection phase is not large enough. Indeed, abrupt phase changes (along the RIS surface) are in general not necessary to manipulate multiple beams generated by the RIS upon a single incident beam, therefore the so called "local periodicty" approximation is generally well accepted. Furthermore, we are in general interested in RIS tuning using a reduced set of degrees of freedom that do not compromise the RIS functionality in the far and Fresnel zones, that involve not abrupt variations of the reflection phase over the RIS. Some full RIS design and practical applications will be presented at the conference.

ACKNOWLEDGEMENT

This material is based upon work supported by the USA National Science Foundation Award 2030029. We also thank Dassault Systèmes for providing CST Studio Suite.

References

[1] A. Pitilakis, et al., "A Multi-Functional Reconfigurable Metasurface: Electromagnetic Design Accounting for Fabrication Aspects," *IEEE Trans. on Antennas and Propagat.*, vol. 69, no. 3, pp. 1440-1454, March 2021.

[2] S. Abeywickrama, R. Zhang, Q. Wu, and C. Yuen, "Intelligent Reflecting Surface: Practical Phase Shift Model and Beamforming Optimization," *IEEE Trans. on Comm.*, vol. 68, no. 9, pp. 5849-5863, Sept. 2020.

[3] Q. Wu, and R. Zhang, "Towards Smart and Reconfigurable Environment: Intelligent Reflecting Surface Aided Wireless Network," *IEEE Communications Magazine*, vol. 58, no. 1, pp. 106-112, Jan. 2020.

[4] C. Huang et al., "Holographic MIMO Surfaces for 6G Wireless Networks: Opportunities, Challenges, and Trends," *IEEE Wireless Communications*, vol. 27, no. 5, pp. 118-125, Oct. 2020.

[5] C. Pan, et al., "Reconfigurable Intelligent Surfaces for 6G Systems: Principles, Applications, and Research Directions," *IEEE Communications Magazine*, vol. 59, no. 6, pp. 14-20, June 2021.

[6] F. Costa, and M. Borgese, "Electromagnetic model of reflective intelligent surfaces," *IEEE Open Jour. of the Comm. Soc.* vol. 2, pp. 1577-1589, 2021.

[7] J. A. Vásquez-Peralvo, J. M. Fernández-González, and J. M. Rigelsford, "Beam Steering Using Active Artificial Magnetic Conductors: A 10-Degree Step Controlled Steering," *IEEE Access*, vol. 8, pp. 177964-177975, 2020.

[8] F. Capolino, A. Vallecchi and M. Albani, "Equivalent Transmission Line Model With a Lumped X-Circuit for a Metalayer Made of Pairs of Planar Conductors," *IEEE Trans. on Antennas and Propagat.*, vol. 61, no. 2, pp. 852-861, Feb. 2013.